Appl. Phys. A (2015) 118:1267–1271
DOI 10.1007/s00339-014-8828-y

Applied Physics A
Materials Science & Processing

High-performance UV photodetectors and temperature-dependent photoluminescence of individual ZnO hexagonal-prism microwire

Meng Ding · Dongxu Zhao · Bin Yao · Qian Qiao · Xijin Xu

Received: 3 June 2014 / Accepted: 13 October 2014 / Published online: 25 October 2014
© Springer-Verlag Berlin Heidelberg 2014

Abstract ZnO hexagonal-prism microwires (HPMs) with the average width of about 50 μm have been fabricated by a floating zone method. Their structural, temperature-dependent photoluminescence (PL) and UV photoresponse based on an individual ZnO HPMs were systematically investigated. For the temperature-dependent PL properties, different transitions including free exciton emission, bound exciton emission and free-to-bound transition were clearly observed at 83 K. The individual ZnO HPM-based UV photodetector showed a response cut-off wavelength of 390 nm and an ultraviolet/visible ratio of about two orders of magnitude with an applied bias of 5 V.

M. Ding · X. Xu (✉)
School of Physics and Technology, University of Jinan, 336 Nanxinzhuang West Road, Jinan 250022, People's Republic of China
e-mail: sps_xuxj@ujn.edu.cn

M. Ding
e-mail: dingmeng0207@163.com

D. Zhao (✉)
State Key Laboratory of Luminescence and Applications, Changchun Institute of Optics, Fine Mechanics and Physics, Chinese Academy of Sciences, 3888 Dongnanhu Road, Changchun 130033, People's Republic of China
e-mail: dxzhao2000@yahoo.com.cn

B. Yao
Department of Physics, Jilin University, Changchun 130023, People's Republic of China

Q. Qiao
School of Naval Architecture and Ocean Engineering, Zhejiang Ocean University, Zhoushan 316000, People's Republic of China

1 Introduction

ZnO with wide band gap (3.37 eV) and larger exciton binding energy (60 meV) has been explored promising applications in short wavelength laser diodes, gas sensor and UV detectors in recent years [1–3]. ZnO with a diverse range of structures and morphologies have been fabricated, and their optical properties of ZnO has also been studied, including stimulated emissions with different kinds of lasing modes at room temperature [4–6]. It is beneficial for defect characterization of the materials with optical characterization methods such as photoluminescence (PL) spectroscopy since it does not require physical contacts. In particular, the low-temperature PL emission peaks are sensitive for the defect states in semiconductors. Furthermore, the study of low-temperature PL of individual ZnO HPM is beneficial to its practical applications in the miniaturization of devices.

ZnO possesses many advantages over other semiconductors as photodetector material, because it exhibits extremely resistant to high-energy proton irradiation and can endure harsh radiation for much longer time, which can be used for space applications. Until now, ZnO-based UV photodetectors, such as the *p*–*n* junction photodiodes and Schottky junction photodiodes, photoconductors have been reported. However, the stable and controllable *p*-type ZnO is difficult to obtain due to the low dopant solubility, the deep acceptor level and the "self-compensation" of shallow acceptors resulting from native donor defects. Therefore, different other *p*-type semiconductors, such as Si, NiO and polymer [7–11] have been chosen to fabricate the *p*–*n* heterojunction UV photodetectors. Some groups have investigated ZnO photoconductors based on films and nanostructure. Different materials have been used as electrodes, including Au, ITO, grapheme, and so on [12–14].

Chang et al. reported the responsivity of interlaced ZnO nanowire UV photodetector was 0.055 A/W, and constant of the photodetectors was 0.447 s [12]. Lupan et al. [15] fabricated single ZnO nanorod-based photodetector using the in-situ lift-out technique. The results showed that the responsivity of the ZnO nanorod was 30 mA/W with the wavelength of 370 nm under an applied bias of 1 V. Li et al. [16] reported the fabrication of a nanowatt UV photodetector with a ultra-long ($\sim$100 μm) ZnO bridging nanowires. The device exhibited drastic current changes (10–10^5 times) under UV irradiations (10^{-8}–10^{-2} W cm^{-2}). The previous preparation of these photodetectors includes some techniques such as photolithography, metal evaporation and dielectric film deposition, which makes the device construction more difficult and complex, and greatly limits the practical applications; however, the photodetector fabricated based on individual ZnO microwire in this work could surmount these difficulties.

In this paper, ZnO HPMs were successfully synthesized by a floating zone method. The temperature-dependent PL spectra ranging from 83 to 293 K were investigated. The individual ZnO HPM-based UV photodetector was simple to obtain, in which the complex procedures like etching, dielectric film deposition can be successfully avoided. Furthermore, the photoconductive properties on the individual ZnO HPM were carefully studied.

2 Experimental

The ZnO HPMs were fabricated by a floating zone method using ZnO powder as the source materials, as previously described [17]. The ZnO HPM-based UV photodetector was assembled as follows. An individual ZnO HPM was selected and fixed by metal indium on the sapphire substrate, in which the metal indium was used as the contact electrode as shown in the inset of Fig. 3. The distance between the two electrodes was about 1 mm.

The morphology of individual as-grown ZnO HPM was characterized by the Field emission scanning electron microscopy (FESEM). The temperature-dependent PL spectra were measured by using a He–Cd laser (325 nm) as excitation source with the testing temperature ranging from 83 to 293 K (model: LabRAM-UV Jobin Yvon). The current versus voltage (I–V) measurements were performed using a Hall measurement system (LakeShore 7707), and the photoconductive properties of an individual ZnO HPM device were measured using a standard lock-in technique with a Xe lamp as an excitation light source, in which all the measurements were performed at room temperature.

3 Results and discussion

The SEM image of an individual ZnO HPM is shown in the inset of Fig. 1, which displays the lateral view of ZnO microwire. Two adjacent surfaces are also observed as labeled 2 and 3. It can be seen that the lateral surfaces are smooth, and the average width is about 50 μm.

The room-temperature PL spectrum of individual ZnO HPM is depicted in Fig. 1, both a sharp and a broad emission peaks can be observed. All the positions of the emission peaks were calibrated by the laser line. The strong ultraviolet emission at 390 nm is clearly observed, which can be attributed to the near band edge emission of ZnO [18]. In addition, the broad emission centered at 525 nm is rather weak compared with the UV emission, which is generally ascribed to structural defects, single ionized vacancies and impurities [19, 20].

The temperature-dependent PL spectra of an individual ZnO HPM ranging from 83 to 293 K are also discussed in details, as shown in Fig. 2. The peak centers at 3.375 eV are dominant at the testing temperature of 83 K, which is ascribed to the recombination of the free exciton (FE) [21, 22]. Meanwhile, a weak emission located at 3.362 eV can be also found at the lower energy shoulder of the FE, is assigned to be shallow donor-bound exciton (D^oX) emission. The D^oX is extrinsic transition and creates discrete electronic states in the band gap. Usually, the impurities and/or shallow donor like defects are the main causes to

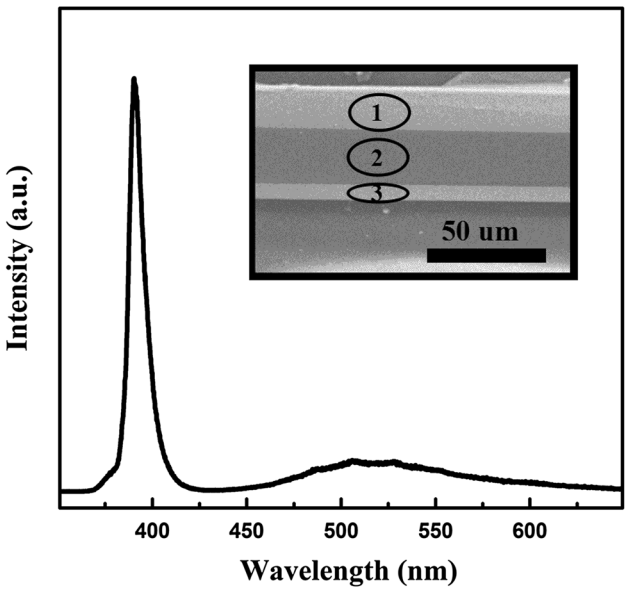

Fig. 1 The room-temperature photoluminescence spectra of the individual ZnO microwire. The inset shows the SEM image of the individual ZnO microwire

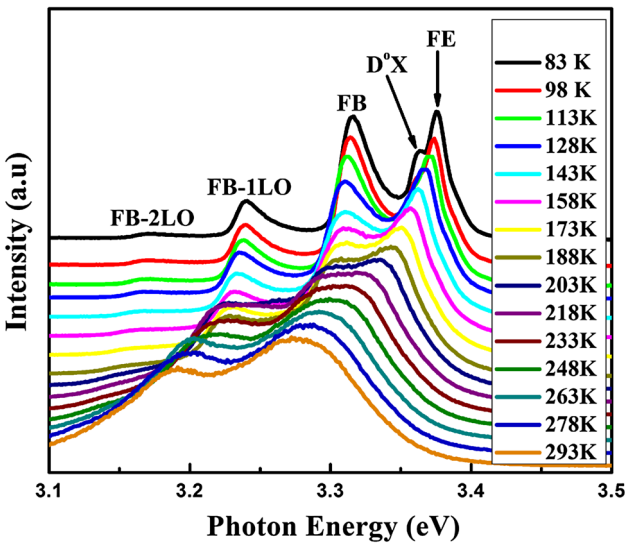

Fig. 2 The temperature-dependent PL spectra of individual ZnO microwire

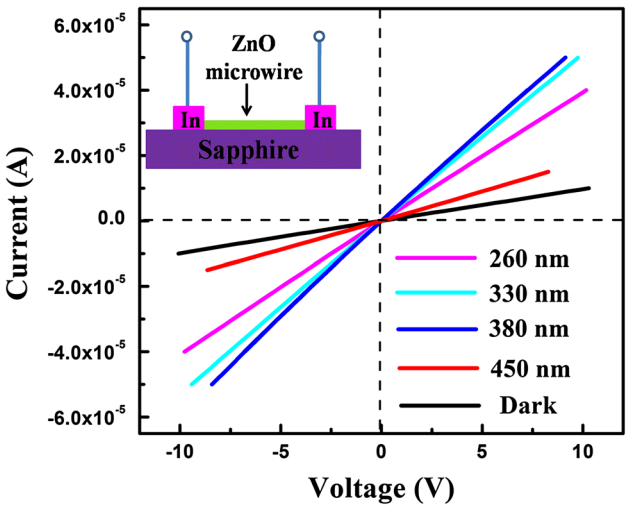

Fig. 3 The *I–V* characteristics of the device illuminated with different wavelength lights and under dark condition. The *inset* shows the schematic diagram of photodetector based on single ZnO microwire

induce the D°X emission [23]. With increasing the testing temperature, the intensity of D°X emission decreases quickly and disappears at 143 K, which may be induced by the thermal dissociation of bound excitons into free excitons due to its small binding energy [24]. Furthermore, the peak positions also show red shift caused by the decrease of ZnO band gap energy with increasing the temperature [25]. The emission located at 3.314 eV is assigned to free-to-bound transition (FB) [26], whose intensities decrease rapidly and finally disappear when the temperature is higher than 248 K due to the decomposition of bound excitons at higher temperature [27]. Finally, the FE peak dominates the spectrum at room temperature. Therefore, the UV emission at 390 nm at room temperature is considered to originate from radiative recombination of free exciton. The Longitudinal optical (LO) phonon replicas occur with a separation of 71–73 meV, as the LO-phonon energy in ZnO [28], so the emissions locating at the lower sides (3.241 and 3.168 eV) of FB can be considered as the corresponding 1-LO, 2-LO phonon replicas of FB, respectively.

Photogenerated carriers can significantly increase the conductivity when a semiconductor material is illuminated by photons with the energy higher than the band gap [29–32]. The schematic diagram of an individual ZnO HPM device is shown in the inset of Fig. 3. The In electrodes were fixed on two ends of the individual ZnO HPM, and the uncovered part of the microwire was exposed to the incident light. Figure 3 shows typical *I–V* curves of an individual ZnO HPM measured under different wavelength light and dark conditions, respectively. It is noticeable that the *I–V* curves are linear and symmetric, which indicate the good ohmic contact between the In electrode and ZnO microwire. The current across the microwire dramatically increases more than six times, from 4.7 (dark condition) to 28.9 μA (with 380 nm light illumination) at a bias voltage of 5.0 V. The obvious increase in photocurrent under these conditions can be understood as follows: When the wavelength of incident light is less than 380 nm, the photon energy is larger than that of the ZnO bandgap, inducing the absorption of light and the generation of and electron–hole pairs, in which the holes can be trapped at the surface. Furthermore, the applied electric filed will lead to the increase of conductivity caused by the collection of the unpaired electrons [33]. When the photon energy increases, the penetration depth of light become shallower, which increases the carrier concentration near the surface; meanwhile, the surface recombination of photogenerated carriers will increase. This is why the photocurrent reduces with the wavelength of incident light decreasing from 380 to 260 nm. When the wavelength of incident light is 450 nm, it has little contribution to photocurrent due to its photon energy smaller than ZnO bandgap, so the photocurrent reduces compared with the wavelength of 380 nm. There is little contribution to photocurrent for the incident light with wavelength of 450 nm due to its photon energy smaller than ZnO, so the photocurrent reduces with the wavelength of incident light from 380 to 450 nm.

The spectral photoresponse of the device at a bias of 5.0 V at wavelengths from 250 to 450 nm is displayed in Fig. 4. The detector shows a high responsivity in the UV spectral region. The peak response is found at 382 nm with a responsivity of about 5.6 mA/W. When the

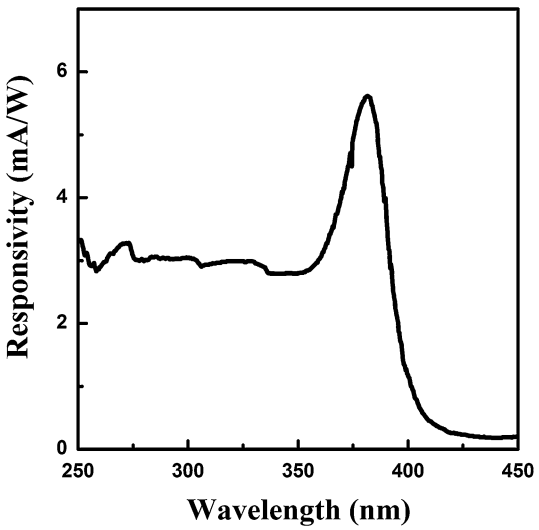

Fig. 4 The spectral response of photodetector based on individual ZnO microwire with an applied bias of 5 V

wavelength decreased, the absorption coefficient increases and the penetration depth of light reduces [34], so the responsivity decreases from 380 to 350 nm. The high photoconductive responsivity may be ascribed to the high photoconductive gain related with the trap states and the surrounding gas molecules [33, 35]. Moreover, a response cut-off wavelength of 390 nm is also observed with an applied bias of 5 V, which is agreement with the result of PL measurement. In addition, the UV/visible rejection ratio (R380/R450 nm) of the photodetector is about two orders of magnitude as shown in the response spectra, which indicates that the photodetector exhibits relatively high signal-to-noise ratio, indicating a high degree of visible blindness. This photoresponse device therefore shows promise as a highly sensitive UV light detector.

The photoresponse of the detector can be explained by the absorption and desorption of oxygen molecules on the surface. Oxygen molecules can be adsorbed on the surface of the oxide and capture the free electrons (O_2-(g) + $e^- \rightarrow O_2^-$(ad)) in the *n*-type semiconductor. The carrier density and mobility of the remaining carriers decrease, so a depletion layer is created and upward band bending near the surface. When the photon with the energy above band gap of ZnO, it can be absorbed; meanwhile, electron–hole pairs are generated ($hv \rightarrow h^+ + e^-$). Holes migrate to the surface along the potential slope due to the band bending and recombine with the O_2-trapped electrons. Therefore, the oxygen is photodesorbed from the surface. The unpaired electrons become the major carriers and collected under an applied electric filed, which leads to the increase in conductivity.

4 Conclusion

In summary, ZnO HPMs have been successfully synthesized by the floating zone method. The emissions related to the FE, shallow donor-bound exciton, FB transition, and its phonon replicas were observed in temperature-dependent PL spectra. The photoconductive device based on individual ZnO microwire was fabricated, and the photodetector showed a response cut-off wavelength of 390 nm and an ultraviolet/visible ratio of about two orders of magnitude with an applied bias of 5 V.

Acknowledgments This work is supported by National Basic Research Program of China (973 Program) under Grant No. 2011CB302004, the National Natural Science Foundation of China (Grant Nos. 11304120, 11304121), the Encouragement Foundation for Excellent Middle-aged and Young Scientist of Shandong Province (Grant Nos. BS2012CL005, BS2013CL020), Doctoral foundation of University of Jinan (UJN) (Grant No. XBS1326). Thanks University of Jinan (UJN) for the support on new staff, and the project supported by the Taishan Scholar (No. TSHW20120210).

References

1. M. Huang, S. Mao, H. Feick, H. Yan, Y. Wu, H. Kind, E. Weber, R. Russo, P. Yang, Science **292**, 1897 (2001)
2. T. Aoki, Y. Hatanaka, D.C. Look, Appl. Phys. Lett. **76**, 3257 (2000)
3. H. Kind, H.Q. Yan, B. Messer, M. Law, P.D. Yang, Adv. Mater. **14**, 158 (2002)
4. M. Ding, D.X. Zhao, B. Yao, S.L. E, Z. Guo, L.G. Zhang, D.Z. Shen, Opt. Express **20**, 13657 (2012)
5. C. Czekalla, C. Sturm, R.S. Grund, B. Cao, M. Lorenz, M. Grundmann, Appl. Phys. Lett. **92**, 241102 (2008)
6. R. Chen, B. Ling, X.W. Sun, H.D. Sun, Adv. Mater. **23**, 2199 (2011)
7. J.J. Qi, X.F. Hu, Z.Z. Wang, X. Li, W. Liu, Y. Zhang, Nanoscale **6**, 6025 (2014)
8. T.C. Zhang, Y. Guo, Z.X. Mei, C.Z. Gu, X.L. Du, Appl. Phys. Lett. **94**, 113508 (2009)
9. H. Ohta, M. Hirano, K. Nakahara, H. Maruta, T. Tanabe, M. Kamiya, T. Kamiya, H. Hosono, Appl. Phys. Lett. **83**, 1029 (2003)
10. Y.Y. Lin, C.W. Chen, W.C. Yen, W.F. Su, C.H. Ku, J.J. Wu, Appl. Phys. Lett. **92**, 233301 (2008)
11. P.N. Ni, C.X. Shan, S.P. Wang, X.Y. Liu, D.Z. Shen, J. Mater. Chem. C **1**, 4445 (2013)
12. S.P. Chang, C.Y. Lu, S.J. Chang, Y.Z. Chiou, T.J. Hsueh, C.L. Hsu, IEEE J. Sel. Top. Quantum Electron. **17**, 990 (2011)
13. B. Nie, J.G. Hu, L.B. Luo, C. Xie, L.H. Zeng, P. Lv, F.Z. Li, J.S. Jie, M. Feng, C.Y. Wu, Y.Q. Yu, S.H. Yu, Small **9**, 2872 (2013)
14. Y.H. Liu, S.J. Young, C.H. Hsiao, L.W. Ji, T.H. Meen, W. Water, S.J. Chang, IEEE Photonics Technol. Lett. **26**, 645 (2014)
15. O. Lupan, L. Chow, G.Y. Chai, L. Chernyak, O.L. Tirpak, H. Heinrich, Phys. Stat. Sol. A **205**, 2673 (2008)
16. Y.B. Li, F.D. Valle, M. Simonnet, I. Yamada, J.J. Delaunay, Nanotechnology **20**, 045501 (2009)
17. X.Y. Guo, Y.N. Yu, D.P. Xu, Z.H. Ding, W.H. Su, Chem. J. Chin. Univ. **27**, 1811 (2006)
18. G.H. Du, F. Xu, Z.Y. Yuan, G.V. Tendeloo, Appl. Phys. Lett. **88**, 243101 (2006)

19. K. Vanheusden, W.L. Warren, C.H. Seager, D.R. Tallant, J.A. Voigt, J. Appl. Phys. **79**, 7983 (1996)
20. G.C. Yi, W.I. Park, Adv. Mater. **14**, 1841 (2002)
21. L. Wischmeier, T. Voss, S. Börner, W. Schade, Appl. Phys. A **84**, 111 (2006)
22. J.S. Jie, G.Z. Wang, Y.M. Chen, X.H. Han, Q.T. Wang, B. Xu, J.G. Hou, Appl. Phys. Lett. **86**, 031909 (2005)
23. Ü. Özgür, Y.I. Alivov, C. Liu, A. Teke, M.A. Reshchikov, S. Doğan, V. Avrutin, S.J. Cho, H. Morkoç, J. Appl. Phys. **98**, 041301 (2005)
24. S.W. Jung, W.I. Park, H.D. Cheong, G.C. Yi, H.M. Jang, S. Hong, T. Joo, Appl. Phys. Lett. **80**, 1924 (2002)
25. Y. Varshni, Physica **34**, 149 (1967)
26. Z. Guo, D.X. Zhao, D.Z. Shen, F. Fang, J.Y. Zhang, B.H. Li, Cryst. Growth Des. **7**, 2294 (2007)
27. W.I. Park, Y.H. Jun, S.W. Jung, G.C. Yi, Appl. Phys. Lett. **82**, 6 (2003)
28. L. Wang, N.C. Giles, J. Appl. Phys. **94**, 973 (2003)
29. T.Y. Zhai, Y. Ma, L. Li, X.S. Fang, M.Y. Liao, Y. Koide, J.N. Yao, Y. Bando, D. Golberg, J. Mater. Chem. **20**, 6630 (2010)
30. T.Y. Zhai, H.M. Liu, H.Q. Li, X.S. Fang, M.Y. Liao, L. Li, H.S. Zhou, Y. Koide, Y. Bando, D. Golberg, Adv. Mater. **22**, 2547 (2010)
31. S.C. Kung, W.E. Van Der Veer, F. Yang, K.C. Donavan, R.M. Penner, Nano Lett. **10**, 1481 (2010)
32. T.Y. Zhai, X.S. Fang, M.Y. Liao, X.J. Xu, H.B. Zeng, Y. Bando, D. Golberg, Sensors **9**, 6504 (2009)
33. C. Soci, A. Zhang, B. Xiang, S.A. Dayeh, D.P.R. Aplin, J. Park, X.Y. Bao, Y.H. Lo, D. Wang, Nano Lett. **7**, 1003 (2007)
34. B. Zhang, X.D. Yang, J.W. Zhang, X.M. Bian, D. Wang, X.N. Zhang, X. Hou, J. Electron. Mater. **38**, 609 (2009)
35. Y.Z. Jin, J.P. Wang, B.Q. Sun, J.C. Blakesley, N.C. Greenham, Nano Lett. **8**, 1649 (2008)